Beach Erosion and Recovery

Nobuhisa Kobayashi, M.ASCE[1]; and Hooyoung Jung[2]

Abstract: Our capability for predicting beach and dune erosion has improved in the last three decades, but the recovery of an eroded beach above the mean sea level (MSL) cannot be predicted at present. The cycle of beach erosion and recovery will need to be predicted for the long-term maintenance of a sand beach with a dune for coastal flooding reduction. The cross-shore numerical model (CSHORE) is extended and evaluated using natural beach erosion and recovery data along 16 cross-shore lines spanning 5 km alongshore for the duration of 272 days. The CSHORE predicts beach and dune erosion fairly well, as has been shown in previous comparisons. The bed-load formula used in the CSHORE is adjusted to predict the accreted beach profile with a berm. The computed beach profile evolutions are shown to be affected little by the alongshore gradient of the longshore sediment transport rate along the straight beach. The extended CSHORE predicts both erosion and accretion above MSL within a factor of about 2. **DOI: 10.1061/(ASCE)WW.1943-5460.0000147.**

CE Database subject headings: Beaches; Sand (hydraulic); Erosion; Storms; Dunes; Predictions.

Author keywords: Beach; Sand; Dune; Erosion; Storm; Recovery.

Introduction

Beach nourishment has been widely adopted in the United States to maintain a wide beach with a high dune and provide coastal storm protection and flooding damage reduction. Numerical models, such as SBEACH (Wise et al. 1996) and XBeach (Roelvink et al. 2009), have been developed to predict storm-induced beach and dune erosion and design the beach and dune profile required for storm protection. XBeach is a horizontally two-dimensional model and has been used to assess storm impact only. XBeach may not predict shoreline accretion under moderate and calm wave conditions (van Thiel de Vries 2009). The amount and frequency of the periodic beach nourishment may increase because of the combined effects of sea level rise and storm intensification because of global warming. The cycle of beach erosion and recovery needs to be predicted to assess the long-term performance of a nourished beach in a changing climate. Presently, the long-term shoreline change is predicted using one-line models, such as GENESIS (Hanson 1989), without regard to beach profile evolution.

The cross-shore numerical model (CSHORE) developed by Kobayashi et al. (2010) consists of the combined wave and current model based on the time-averaged continuity, momentum, and wave energy equations coupled with the transparent formulas for suspended sand and bed-load transport rates, which have been shown to synthesize available sediment transport data and formulas. The CSHORE includes a probabilistic model for the wet and dry zone above the shoreline to predict dune erosion and overwash as well as longshore sediment transport in the swash zone. The CSHORE has been compared with a number of small-scale and large-scale laboratory data as well as field data. However, these comparisons do not include the recovery above mean sea level (MSL) of eroded beaches after storms. The computations for field data on beach and dune erosion were limited to the storm duration only, even though the beach profiles were measured well before the storm and about a week after the storm. In this study, the CSHORE is compared with the entire duration of beach erosion and recovery data from the Atlantic coast in Delaware. In addition, the CSHORE is extended to multiple cross-shore lines, and therefore the alongshore gradient of the longshore sediment transport rate in the beach profile evolution prediction is included.

In the subsequent paragraphs, the field data are presented first. The existing model CSHORE is described concisely, and the modifications of CSHORE are presented. The modified CSHORE is compared with the field data and the sensitivities of the computed profiles to the modifications are assessed. Finally, the findings of this study are summarized. This paper presents the essential parts of the report by Jung and Kobayashi (2011).

Field Data

The Atlantic sandy coast of 40-km length in Delaware is suffering from chronic beach erosion and has been maintained by periodic beach nourishment for the last two decades (Figlus and Kobayashi 2008). This study is limited to 16 beach profiles at Rehoboth and Dewey beaches, as depicted in Fig. 1. These 16 profiles were measured on October 29, 1992, December 18, 1992, and July 27, 1993, before the major nourishment of these beaches in 1994 (Garriga and Dalrymple 2002). These profile data indicate the cycle of erosion and recovery of the natural beaches. The beach sand was fairly well sorted. and its median diameter was 0.33 mm. Data from the tide gauge at Lewes, Delaware in Fig. 1 is used to specify the hourly variation of the water level. A wave gauge (DE001 in Fig. 1) was located at a depth of about 9 m off the coast of Dewey Beach. The time series of the root-mean-square wave height H_{rms}, spectral peak period T_p, and peak spectral wave direction θ are available every 4 hours. The available time series are interpolated to obtain the hourly time series corresponding to the hourly water level data.

[1]Professor and Director, Center for Applied Coastal Research, Univ. of Delaware, Newark, DE 19716 (corresponding author). E-mail: nk@udel.edu

[2]Graduate Student, Dept. of Civil and Environmental Engineering, Univ. of Delaware, Newark, DE 19716.

Note. This manuscript was submitted on June 10, 2011; approved on February 24, 2012; published online on February 27, 2012. Discussion period open until April 1, 2013; separate discussions must be submitted for individual papers. This paper is part of the ***Journal of Waterway, Port, Coastal, and Ocean Engineering***, Vol. 138, No. 6, November 1, 2012. ©ASCE, ISSN 0733-950X/2012/6-473–483/$25.00.

J. Waterway, Port, Coastal, Ocean Eng. 2012.138:473-483.

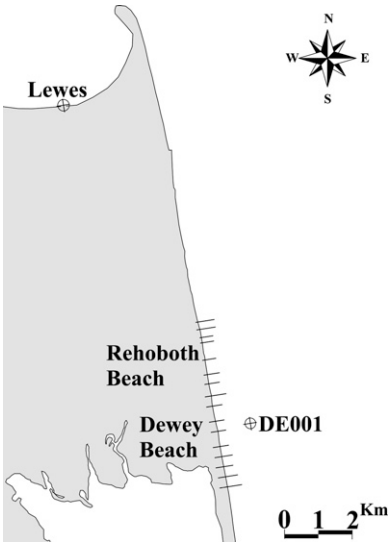

Fig. 1. Rehoboth Beach, Dewey Beach, 16 cross-shore survey lines, Lewes Tide Gauge, and Wave Gauge DE001

Table 1. Average Water Level and Wave Conditions during Erosion and Accretion Periods

Period	Erosion	Accretion
Start date	October 29, 1992	December 18, 1992
End date	December 18, 1992	July 27, 1993
Number of days	50.80	220.80
Average water level (m)	0.17	0.13
Average H_{rms} (m)	0.81	0.59
Average T_p (s)	9.40	8.30
Average wave angle θ (degrees)	8.50	8.50

A storm attacked Rehoboth (R) and Dewey (D) Beaches on December 10, 1992. The comparison of the beach profiles measured on October 29, 1992, and December 18, 1992, indicated considerable erosion above the MSL for the 16 profiles. The eroded beaches recovered almost completely when the 16 profiles were measured on July 27, 1993. The erosion and accretion periods analyzed are summarized in Table 1, which lists the average values of the water level above the MSL, H_{rms}, T_p, and θ during each period. The wave angle is taken to be positive clockwise from the normal to the straight shoreline inclined at an angle of 8.86° counterclockwise from the north. The net longshore sediment transport along these beaches is northward.

Fig. 2 shows the measured time series of the water level, H_{rms}, T_p, and θ during the erosion period where the abscissa is the number of days since October 29, 1992. The horizontal line in each panel is the average value listed in Table 1. The storm of December 10, 1992, lasted about 4 days with a peak water level of almost 2 m, a peak wave height of almost 3 m, wave periods of about 15 s, and wave directions of about 20°. The measured time series of the water level, H_{rms}, T_p, and θ for the accretion period indicated several minor storms with a peak water level of about 1 m, a peak wave height of about 2 m, and a storm duration of 1−2 days. The water level, wave height, and duration of these minor storms were clearly less than those of the major storm during the erosion period. The entire time series of the water level, H_{rms}, T_p, and θ are specified as input at the seaward boundary of the CSHORE in the water depth of about 9 m in order to simulate the beach profile evolution for the entire erosion

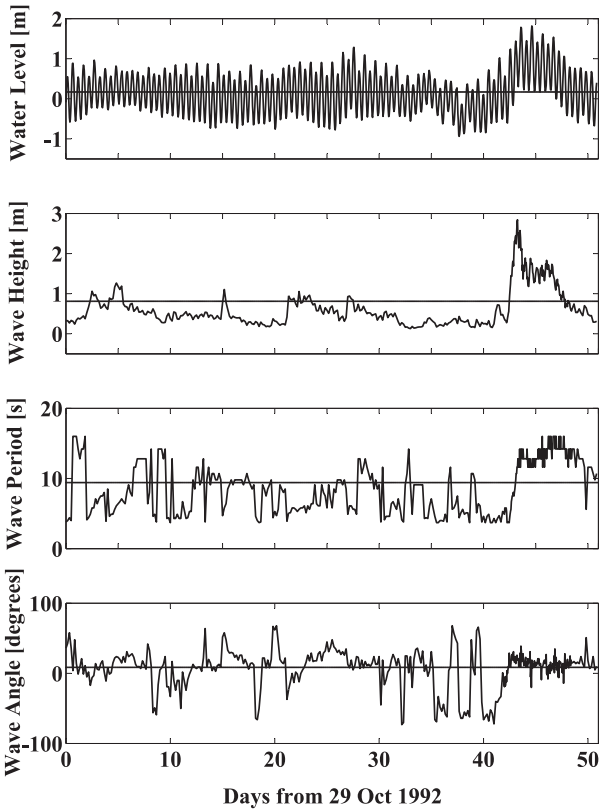

Fig. 2. Water level, root-mean-square wave height, spectral peak period, and peak spectral wave direction during erosion period

and accretion periods. The alongshore variation of the wave conditions was assumed to be negligible.

The three beach profiles along each of the 16 cross-shore lines measured on October 29, 1992, December 18, 1992, and July 27, 1993, are plotted together to determine the cross-shore overlapping zone of the three profiles along each cross-shore line. The onshore coordinate x along each cross-shore line is taken as $x = 0$ at the seaward boundary of the CSHORE and $x = x_m$ at the landward boundary of the overlapping zone above the MSL. The values of x_m among the 16 profiles varied in the range of 309−634 m, and the average value of x_m was 417 m. During the erosion period, erosion and deposition occurred above and below the MSL, respectively, and the shoreline location at the MSL did not vary much. During the accretion period, accretion and erosion occurred above and below MSL, respectively, and the beach profile at the beginning of the erosion period was similar to the corresponding profile at the end of the accretion period. The measured profiles are subsequently presented when they are compared with the computed profiles using the CSHORE. The shoreline location did not represent the observed erosion and accretion on these beaches.

Table 2 summarizes the profile data for R and D Beaches where N and S indicate the northern and southern segments of each beach. The numeral after N or S is related to the alongshore distance from the middle (numeral = 0) of each beach. The alongshore coordinate y is taken to be positive northward in the direction of the net longshore sediment transport with $y = 0$ at the most southern line DS40. The landward extent of some of the overlapped profiles was too short to resolve the dune profile change adequately. The sand volume per unit alongshore length above the MSL is calculated using the beach profile measured on October 29, 1992, for each line to indicate the relatively large alongshore variation of the beach profile above the

J. Waterway, Port, Coastal, Ocean Eng. 2012.138:473-483.

Table 2. Sand Volume per Unit Alongshore Length above Mean Sea Level on October 29, 1992, Erosion Volume above Mean Sea Level during Erosion Period, and Accretion Volume above Mean Sea Level during Accretion Period Where Sand Volume Include Voids

Line	y (m)	x_m (m)	Sand volume (m^3/m)	Erosion volume (m^3/m)	Accretion volume (m^3/m)
RN38	4,975	479	162	49	43
RN31	4,750	466	200	59	59
RN22	4,504	379	73	37	38
RN17	4,345	355	80	42	49
RS0	3,830	309	102	50	56
RS14	3,389	363	142	66	77
RS24	3,112	400	166	65	64
RS36	2,744	575	302	91	77
DN40	2,439	391	227	63	64
DN25	1,982	331	93	68	77
DN15	1,677	326	80	56	52
DN0	1,220	359	89	67	86
DS10	915	374	87	68	70
DS20	610	411	173	72	62
DS30	305	520	138	72	58
DS40	0	634	194	75	56

MSL. The erosion volume per unit length above the MSL is calculated using the measured profiles at the beginning and end of the erosion period. The accretion volume per unit length above the MSL is calculated using the measured profiles at the beginning and end of the accretion period. The erosion and accretion volumes were similar and did not vary alongshore as much as the initial sand volume. The erosion and accretion above the MSL were more uniform alongshore than the initial 16 beach profiles.

Numerical Model

The CSHORE assumes unidirectional irregular waves and alongshore uniformity along each cross-shore line. The hydrodynamic model in the CSHORE predicts the mean and standard deviation of the free surface elevation above the still water level and depth-averaged cross-shore and longshore velocities. The time-averaged continuity, cross-shore momentum, longshore momentum, and wave energy equations together with Snell's law are used in the wet zone seaward of the still water shoreline (Kobayashi et al. 2007), where the roller effect is found to be negligible in the present profile evolution comparison and is not included in the following computed results. The breaker ratio parameter γ is taken as its typical value of $\gamma = 0.7$, where the computed profile evolution is not sensitive to $\gamma = 0.7$ or 0.8. The bottom friction factor f_b is taken as $f_b = 0.02$, calibrated for longshore current and sediment transport by Kobayashi et al. (2007). In the wet and dry zone, the wave angle was assumed to be small and remain the same as the wave angle at the still water shoreline. The time-averaged continuity and cross-shore momentum equations are used together with the wet probability for the presence of water (Kobayashi et al. 2010).

The sediment transport model in the CSHORE consists of separate formulas for bed load and suspended load. The volume of suspended sediment per unit bottom area was expressed in terms of the wave energy dissipation rates because of wave breaking and bottom friction (Kobayashi et al. 2008). The suspended sediment is assumed to be transported by the cross-shore and longshore currents (Kobayashi et al. 2007). The effect of onshore flow because of wave overtopping is included to estimate the cross-shore suspended sediment transport rate q_{sx} (Figlus et al. 2011), where the wave overwash parameter a_o is taken as $a_o = 0.1$, but the computed profile evolution is not very sensitive to a_o in the range of 0.1−1.0. The longshore suspended sediment transport rate q_{sy} is proportional to the longshore current which is sensitive to the bottom friction factor $f_b = 0.02$ assumed in the following.

The cross-shore and longshore bed-load transport rates q_{bx} and q_{by} are expressed as a function of the mean and standard deviation of the cross-shore and longshore velocities (Kobayashi et al. 2009). The effect of the cross-shore bottom slope on q_{bx} was included to reduce the onshore bed-load transport rate q_{bx} on a steep upward slope. The rates q_{bx} and q_{by} are proportional to the empirical bed-load parameter b. Kobayashi et al. (2008) calibrated b using 20 water tunnel tests, 4 large-scale wave flume tests, and 24 sheet flow tests. The calibrated range for these tests with nonbreaking waves on horizontal bottoms was $b = 0.001-0.004$, and the typical value of $b = 0.002$ has been used to predict beach and dune erosion for which offshore suspended sediment transport is dominant. The parameter b needs to be calibrated for beach accretion in the surf and swash zones. For the present comparison with the beach erosion and recovery data, $b = 0.002$ was found to reproduce the 16 eroded profiles as well as for the previous comparisons (Kobayashi et al. 2010) but could not reproduce the 16 accreted profiles because of the deposition near the shoreline at the MSL, unlike the observed upward berm reconstruction above the MSL. To cause the landward increase of the onshore bed-load transport rate q_{bx}, use is made of $b = B(0.5 + Q)$ with $B = 0.002$ where the computed fraction Q of irregular breaking waves is zero for no wave breaking and unity when all waves break. Consequently, b increases from 0.001 outside the surf zone to 0.003 near the still water shoreline in the wet zone and in the swash zone. The sensitivity of the computed profile change to the input value of B is presented after the comparison using $B = 0.002$.

The cross-shore beach profile evolution along each of the 16 lines is predicted using the continuity equation of bottom sediment

$$(1 - n_p)\frac{\partial z_b}{\partial t} + \frac{\partial q_x}{\partial x} + \frac{\partial q_y}{\partial y} = 0 \tag{1}$$

where n_p = porosity of bottom sediment assumed as $n_p = 0.4$; t = morphological time; z_b = bottom elevation with $z_b = 0$ at the MSL; q_x = total cross-shore sediment transport rate per unit width given by $q_x = (q_{sx} + q_{bx})$; and q_y = total longshore sediment transport rate per unit width given by $q_y = (q_{sy} + q_{by})$. The alongshore gradient of q_y is included in Eq. (1) in order to allow the gradual alongshore variation of longshore sediment transport, although the alongshore uniformity is assumed for each cross-shore line. The CSHORE is modified to allow the simultaneous computation of the multiple cross-shore lines and includes the effect of the alongshore gradient of q_y on the temporal variation of z_b along each line in approximate but computationally efficient manners.

To solve Eq. (1) numerically, the bottom elevation z_b is expressed as $z_b = (z_x + z_y)$, and Eq. (1) is rewritten as

$$(1 - n_p)\frac{\partial z_x}{\partial t} + \frac{\partial q_x}{\partial x} = 0 \tag{2}$$

$$(1 - n_p)\frac{\partial z_y}{\partial t} + \frac{\partial q_y}{\partial y} = 0 \tag{3}$$

Eq. (2) is solved using the same numerical method as that used for the case of no alongshore gradient of q_y in Eq. (1) (Kobayashi et al. 2007). Eq. (3) is integrated with respect to time t for the duration of

J. Waterway, Port, Coastal, Ocean Eng. 2012.138:473-483.

constant water level and wave conditions where $\Delta t = 1\,h$ in the present computation. The bottom elevation change Δz_y is expressed as

$$(1 - n_p)\Delta z_y + \frac{\partial v_y}{\partial y} = 0, \quad v_y = \int_t^{t+\Delta t} q_y dt \tag{4}$$

where v_y = longshore sediment transport volume per unit width for the duration of Δt, which is obtained during the computation of z_x. The value of Δz_y based on Eq. (4) is added to the bottom elevation z_x computed using Eq. (2) at the interval of Δt. This numerical procedure assumes that the time scale of z_x in Eq. (2) is smaller than that of z_y in Eq. (3). This procedure is also convenient because the time step size used to solve Eq. (2) is constrained by the numerical stability criterion and can vary among the cross-shore lines.

The alongshore length scale is assumed to be larger than the cross-shore length scale in order to be consistent with the profile layout in Table 2, where the spacing of the cross-shore lines is as large as the cross-shore distance x_m. No additional cross-shore line is added to estimate the alongshore gradient of v_y in Eq. (4), which is expressed as

$$\frac{\partial v_y}{\partial y} = \frac{1}{L_x}\frac{\partial V_y}{\partial y}, \quad V_y = \int_0^{x_m} v_y dx, \quad \int_0^{x_m} \frac{dx}{L_x} = 1 \tag{5}$$

where V_y = longshore sediment transport volume across the entire cross-shore line, and L_x = cross-shore length related to the cross-shore variation of Δz_y in view of Eq. (4). If $L_x = x_m$ is assumed, the alongshore gradient of V_y causes the uniform change of Δz_y across the cross-shore line.

The cross-shore length scale L_x is assumed to be related to the cross-shore profile change

$$L_x = \frac{A_x}{|\Delta z_x|}, \quad A_x = \int_0^{x_m} |\Delta z_x|\, dx \tag{6}$$

where Δz_x = bottom elevation change based on Eq. (2) during time t to $(t + \Delta t)$. Eq. (6) satisfies the requirement of L_x in Eq. (5). Substitution of Eqs. (5) and (6) into Eq. (4) yields

$$\Delta z_y = \frac{-|\Delta z_x|}{(1 - n_p)A_x}\frac{\partial V_y}{\partial y} \tag{7}$$

which shows that Δz_y is proportional to the magnitude of the bottom elevation change Δz_x because of the cross-shore sediment transport. This eliminates the need to specify the seaward and landward limit of the profile change for one-line models. The sign (accretion or erosion) of Δz_y in Eq. (7) depends on the alongshore gradient of V_y and remains the same along the cross-shore line. The alongshore gradient of V_y is approximated by an upstream differencing method (Anderson et al. 1984) for its numerical stability where the upstream direction is determined by the direction of V_y. Eq. (6) may not be rigorous but allows the use of a large alongshore spacing of two adjacent cross-shore lines.

The input to the CSHORE includes the hourly time series of the water level above the MSL and the incident wave conditions represented by H_{rms}, T_p, and θ at the seaward boundary $x = 0$. Wave setup is assumed to be zero at $x = 0$. The beach sand is characterized by the median diameter of 0.33 mm and the fall velocity of 5 cm/s. The initial beach profile at time = 0 was the measured profile along each of the 16 cross-shore lines on October 29, 1992, for the erosion period and that on December 18, 1992, for the accretion period to assess the capability and limitation of the CSHORE for predicting beach erosion and recovery separately. The cross-shore nodal spacing is 3 m for each cross-shore line. The computation time was 9 min for the erosion period of 50.8 days and 30 min for the accretion period of 220.8 days. The short computation time facilitated the modifications of the CSHORE, which required a number of trial computations.

Comparison of Numerical Model with Field Data

The measured and computed profiles at the end of each period are compared for each of the 16 lines. The comparisons at RN38 (northern end), DS10 (dune overwash zone), and DS40 (southern end) in Table 2 are presented in the subsequent paragraphs to represent the alongshore variation of the agreement among the 16 lines. The computed rates q_{bx}, q_{sx}, q_x, q_{by}, q_{sy}, and q_y are integrated with time to obtain the cumulative sediment volumes per unit width transported during each period and to examine the computed cross-shore and longshore sediment transport.

The measured initial profile and the measured and computed profiles at the end of the erosion period are presented in the top panel of Figs. 3, 4, and 5. The elevation z is zero at the MSL. The offshore zone of the negligible profile change is omitted in these figures. The eroded berm and dune profile is predicted well for RN38 in Fig. 3. Dune overwash occurred at DS10 in Fig. 4, but the measured profile did not extend sufficiently landward. Dune overwash also occurred at DN0 located 305 m north of DS10. The eroded profile above MSL at DS10 is underpredicted partly because of the boundary condition of zero cross-shore gradient of q_x at $x = x_m$ used to solve Eq. (2). The accreted profile below MSL may be related to the erosion above MSL, but its cause is not certain for lack of the landward profile data because the eroded sand must have also been transported landward. The erosion of the berm and dune at DS40 in Fig. 5 is underpredicted, and the nearly horizontal eroded profile near MSL cannot be predicted by the CSHORE.

The cumulative cross-shore sediment volumes per unit width transported during the erosion period are plotted in the middle panel of Figs. 3–5. The CSHORE predicts the onshore (positive) bed-load transport and the offshore (negative) suspended load transport for the case of negligible wave overwash. The total load is the sum of bed load and suspended load. The onshore bed load and offshore suspended load are computed to be of similar magnitude and the maximum near the MSL. The small total load is plotted in Fig. 6, where small fluctuations occur near and above the MSL. For RN38 and DS40 with no or minor dune overwash, the offshore total load was the maximum near the MSL and approaches zero landward. The CSHORE predicts the small onshore sediment transport outside the surf zone where the onshore bed-load transport was predicted to exceed the offshore suspended sediment transport. This onshore sediment transport rate varies gradually in the cross-shore direction and causes very small profile changes. For DS10 with major dune overwash, the total load was small seaward of the MSL and increases landward of the MSL because of the onshore flow associated with dune overwash.

On the other hand, the cumulative longshore sediment volumes per unit width transported during the erosion period are plotted in the bottom panel of Figs. 3–5. The net longshore transport of bed load and suspended load was positive and northward along the Delaware Atlantic coast. The suspended load was dominant for the longshore sediment transport and the maximum near the MSL. The CSHORE has been shown to predict the cross-shore distribution of longshore sediment transport under constant water level and wave conditions (Kobayashi et al. 2007). The large longshore sediment transport in the swash zone explains the maximum cumulative load near the MSL.

An option is provided in the CSHORE to compute the beach profile change without (IQYDY = 0) and with (IQYDY = 1) the

J. Waterway, Port, Coastal, Ocean Eng. 2012.138:473-483.

correction term given by Eq. (7). The computed bottom elevation z_b at the end of the erosion period for IQYDY = 0 is subtracted from that for IQYDY = 1. The elevation difference indicates the effect of the alongshore gradient of the longshore sediment transport on the cross-shore profile change. The computed elevation difference shown in Fig. 7 turns out to be of the order of 10 cm or less in the zone of the profile changes in Figs. 3–5. The positive (negative) elevation difference implies accretion (erosion) because of the longshore sediment transport gradient. The cross-shore variation of the elevation difference depends on the length scale L_x, which is assumed to be given by Eq. (6). The computed elevation difference is much smaller than the profile changes of the order of 1 m or more in Figs. 3–5.

Figs. 8, 9, and 10 show the comparison at the end of the accretion period for RN38, DS10, and DS40, respectively. The CSHORE cannot reproduce the berm sufficiently for RN38 and DS10 but predicts the accreted profile at DS40 well. The effect of the alongshore gradient of the longshore sediment transport was quantified by computing the elevation difference in the same way as in Fig. 7. The computed elevation difference was less than 5 cm and small for the accretion period as well. The dune at DS10 (dune overwash zone) on July 27, 1993, may be related to the emergency nourishment of 4,400 m^3 in July 1993 (Garriga and Dalrymple 2002), which is not included in the computed profile for lack of the fill placement information. Assuming the placement of 4,400 m^3

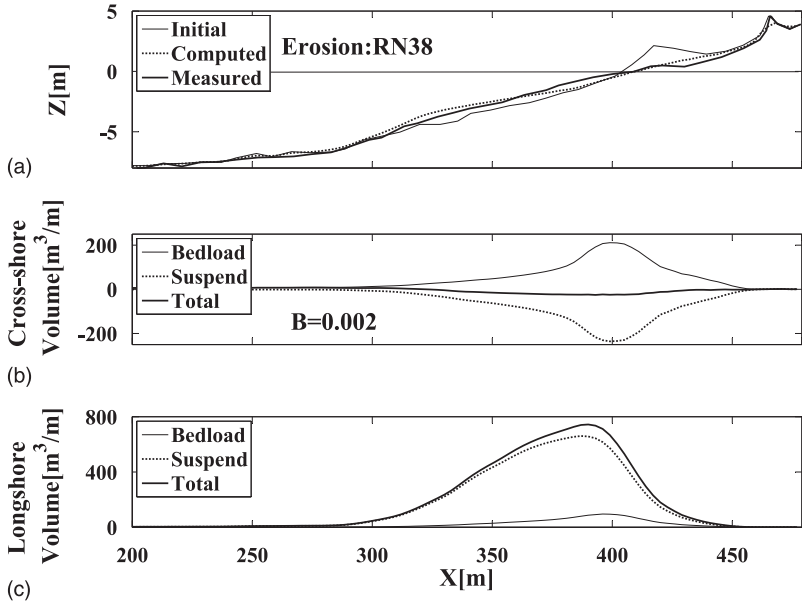

Fig. 3. Measured and computed (a) beach profiles, (b) cumulative cross-shore, and (c) longshore sand transport volume per unit width during erosion period for RN38

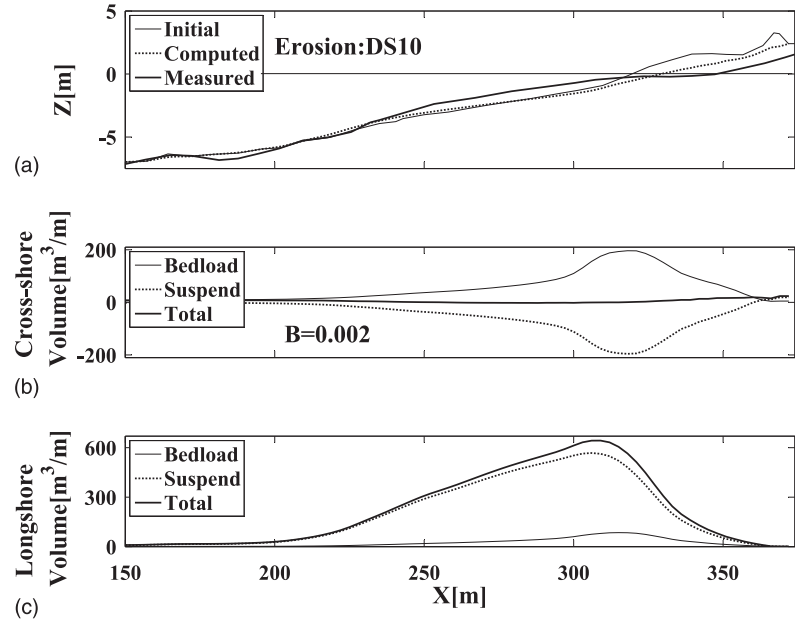

Fig. 4. Measured and computed (a) beach profiles, (b) cumulative cross-shore, and (c) longshore sand transport volume per unit width during erosion period for DS10

J. Waterway, Port, Coastal, Ocean Eng. 2012.138:473-483.

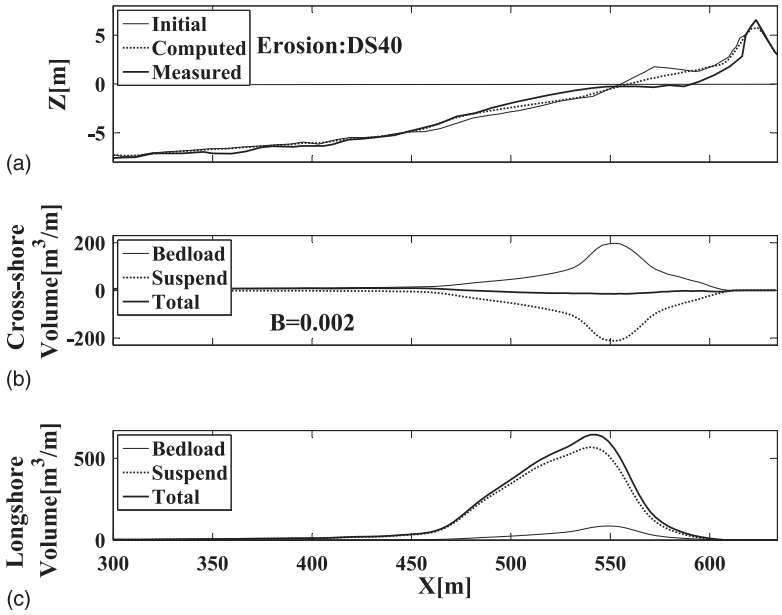

Fig. 5. Measured and computed (a) beach profiles, (b) cumulative cross-shore, and (c) longshore sand transport volume per unit width during erosion period for DS40

between DN0 and DS10 with the alongshore distance of 305 m, the placement volume per unit length is 14 m^3/m, which is small in comparison with the accretion volume per unit length of 86 and 70 m^3/m at DN0 and DS10, respectively, as listed in Table 2. Wind-blown sediment transport (U.S. Army Engineer Research and Development Center 2002) may not be negligible for the accretion period of 220.8 days.

The cumulative cross-shore bed load and suspended load in the middle panel of Figs. 8–10 are larger than those in Figs. 3–5 for the erosion period of 50.8 days. The cumulative cross-shore total load appears to be almost zero in these figures and is plotted separately in Fig. 11. The total load is positive (onshore) and the maximum near MSL is even at DS10. The magnitude of the onshore total load in Fig. 11 is similar to the magnitude of the offshore total load in Fig. 6. This explains the recovery of the eroded profile. The sum of the onshore total load at $x = 0$ (about 9-m depth) in Figs. 6 and 11 is about 15 m^3/m for the duration of 272 days and of the same order of magnitude as the onshore sediment transport rate of 5–10 m^3/m per year in 20-m depth in Holland, estimated by van Rijn (1997). On the other hand, the cumulative longshore bed load, suspended load, and total load in the bottom panel in Figs. 8–10 are similar in their magnitudes to those in Figs. 3–5 for the erosion period, but the cross-shore extent is narrower for the accretion period with smaller wave heights, as indicated in Table 1.

The computed results shown in Figs. 3–11 are based on the bed load parameter $b = B(0.5 + Q)$ with $B = 0.002$. The onshore bed-load transport rate is proportional to the value of B specified as input to the CSHORE. Fig. 5 for DS40 indicates that $B = 0.002$ does not produce sufficient erosion above the MSL. The computed results with $B = 0.001$ are shown in Fig. 12. The reduction of B by the factor of 2 reproduces the eroded profile above the MSL, but the offshore deposition is overpredicted. The cumulative cross-shore and longshore bed-load volumes per unit width are reduced by the factor of more than 2, but the corresponding suspended load volumes are reduced as well. This is because the modified bed load changes the beach profile, which affects the computed hydrodynamics and the offshore transport of suspended sediment by undertow current. The hydrodynamics, sediment dynamics, and beach profile changes are closely interconnected for the beach profile evolution.

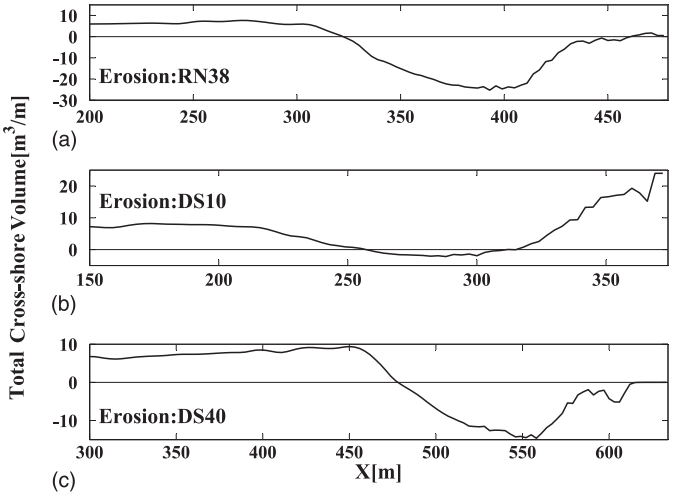

Fig. 6. Cumulative total cross-shore sand transport volume per unit width during erosion period for (a) RN38, (b) DS10, and (c) DS40

Fig. 13 shows the computed results with $B = 0.003$ for RN38 in comparison with those with $B = 0.002$ shown in Fig. 8. The increase of B by the factor of 1.5 increases accretion above the MSL and the cumulative bed load and suspended load. The value of $B = 0.003$ improves the agreement for the accretion volume per unit width above the MSL, but the accretion occurs on the seaward side of the shoreline at the MSL instead of the upward berm reconstruction. This computed profile looks similar to the accreted profile predicted using $b = B$ with $B = 0.002$ before the present modification of $b = B(0.5 + Q)$. The reproduction of the accreted profile above the MSL is found to be more difficult than that of the eroded profile above the MSL.

Fig. 14 compares the computed erosion and accretion volumes per unit alongshore length above the MSL for the 16 lines with the

J. Waterway, Port, Coastal, Ocean Eng. 2012.138:473-483.

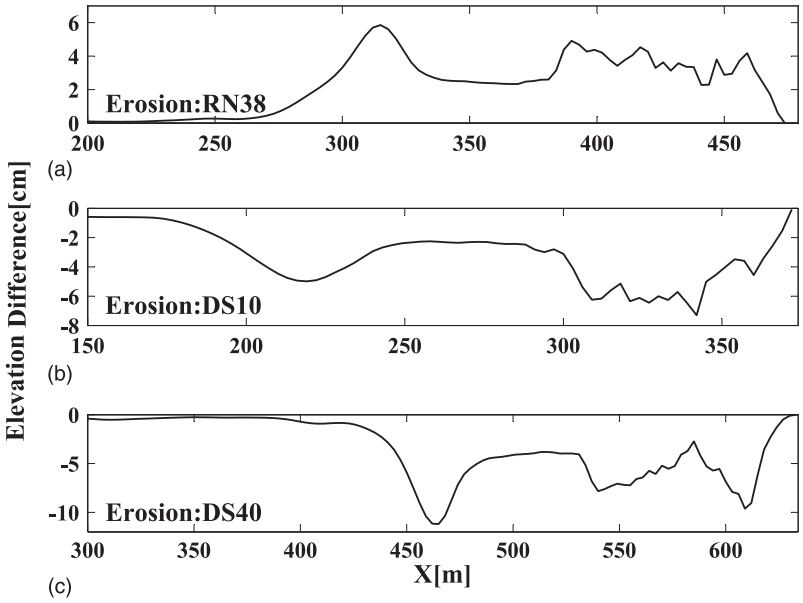

Fig. 7. Bottom elevation difference on December 18, 1992, caused by alongshore gradient of longshore sediment transport rate for (a) RN38, (b) DS10, and (c) DS40

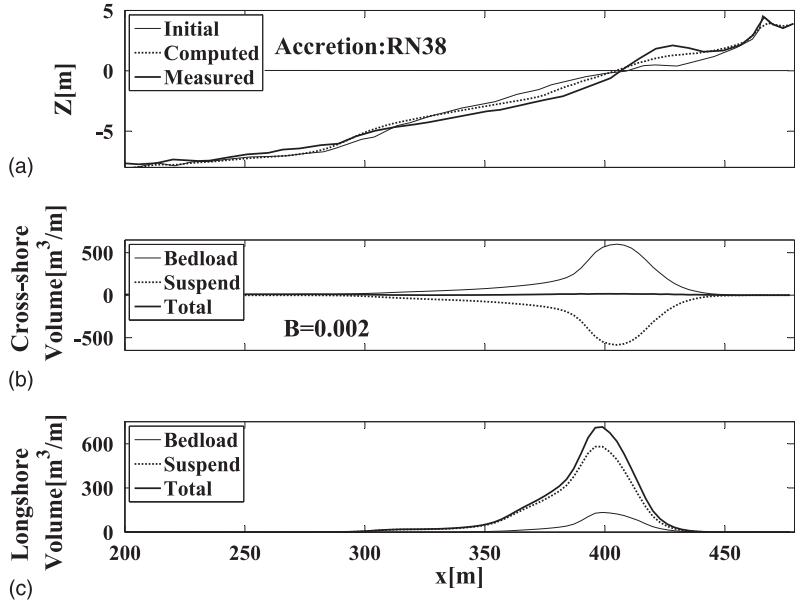

Fig. 8. Measured and computed (a) beach profiles, (b) cumulative cross-shore, and (c) longshore sand transport volume per unit width during accretion period for RN38

measured values listed in Table 2, where RN38 and DS40 are located at the alongshore coordinate $y = 4{,}975$ m and $y = 0$, respectively. First, the computed volumes for $B = 0.002$ are compared with the measured volumes. The erosion volume is predicted well in the N segment of R Beach. The underprediction of the erosion volume increases southward. On the other hand, the alongshore variation of the agreement for the accretion volume is opposite. The agreement is good at the S end of D Beach, but the underprediction persists northward. The computed results account for the initial profile differences among the 16 lines, but the offshore wave conditions at $x = 0$ are assumed to be invariant alongshore. The erosion volume is predicted better for $B = 0.001$, which cannot predict accretion. The accretion volume is predicted better for $B = 0.003$, which cannot predict erosion. The use of $B = 0.002$ predicts the erosion and accretion volumes within a factor of about 2. The accurate prediction of both erosion and accretion is difficult because of the small difference between the onshore bed-load transport and the offshore suspended sediment transport.

The cumulative total sediment volume per unit width transported alongshore and northward is integrated from $x = 0$ to $x = x_m$ to obtain the sediment volume (no void) transported during the erosion and accretion periods. Fig. 15 shows the computed sediment volumes for the 16 lines for $B = 0.001$, 0.002, and 0.003. The longshore sediment transport is less sensitive to the parameter B for bed load. The computed volume of sediment transported alongshore increases somewhat in the S segment of D Beach and fluctuates slightly

J. Waterway, Port, Coastal, Ocean Eng. 2012.138:473-483.

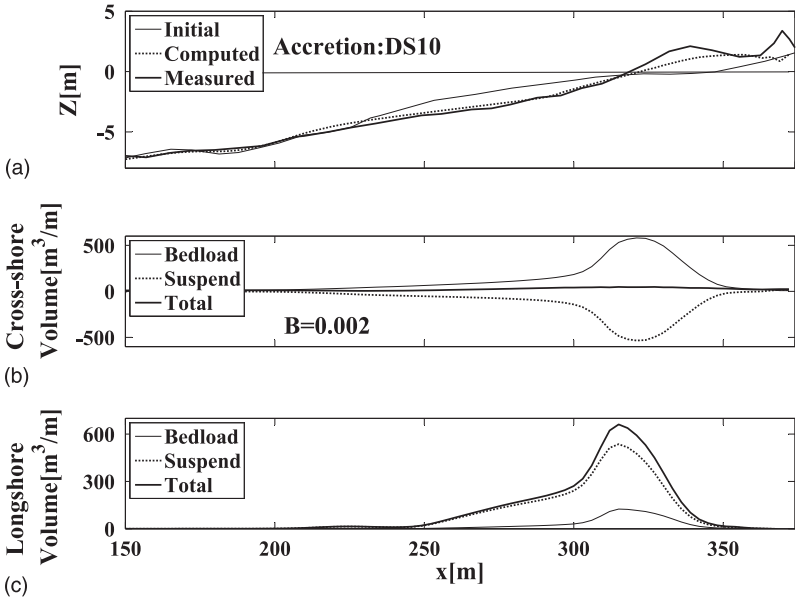

Fig. 9. Measured and computed (a) beach profiles, (b) cumulative cross-shore, and (c) longshore sand transport volume per unit width during accretion period for DS10

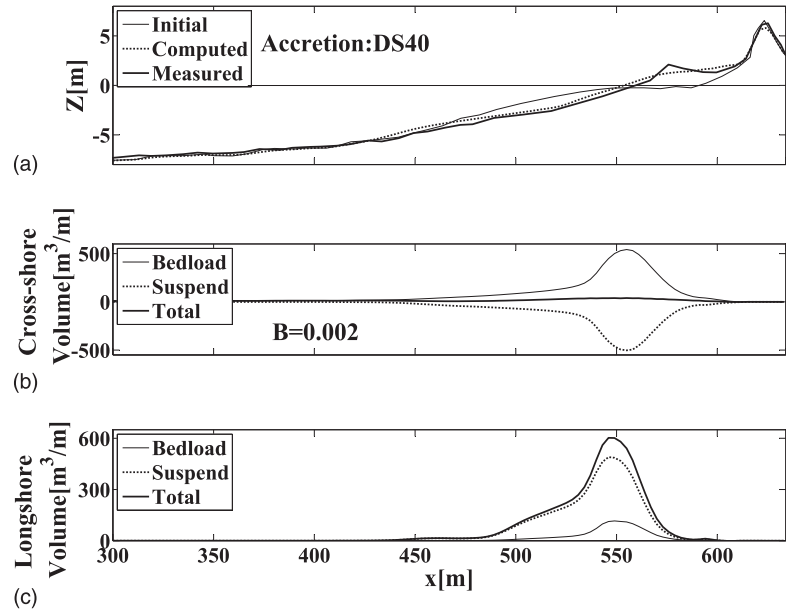

Fig. 10. Measured and computed (a) beach profiles, (b) cumulative cross-shore, and (c) longshore sand transport volume per unit width during accretion period for DS40

northward during the erosion period. The erosion and accretion in the computed elevation differences in Fig. 7 are consistent with this alongshore variation. The computed sediment volume was almost constant during the accretion period. For $B = 0.002$, the average sediment volume transported alongshore is 5.4×10^4 m^3 during the erosion period of 50.8 days and 2.6×10^4 m^3 during the accretion period of 220.8 days. The annual net longshore sediment (no void) transport rate has been estimated to be of the order of 6×10^4 m^3/year to the north (Puleo 2010), where the sand porosity is assumed to be 0.4. The longshore sediment transport rate predicted by the CSHORE is of the same order as the previous estimate, partly because of the use of the bottom friction factor $f_b = 0.02$ calibrated using two data sets obtained in the Large-Scale Sediment Transport Facility of the U.S. Army Engineer Research and Development Center (Kobayashi et al. 2007). The bottom friction factor affects longshore current and suspended sediment transport.

Conclusions

Beach profile data from R and D Beaches are analyzed to examine the cycle of beach erosion and recovery during 1992−1993 before

J. Waterway, Port, Coastal, Ocean Eng. 2012.138:473-483.

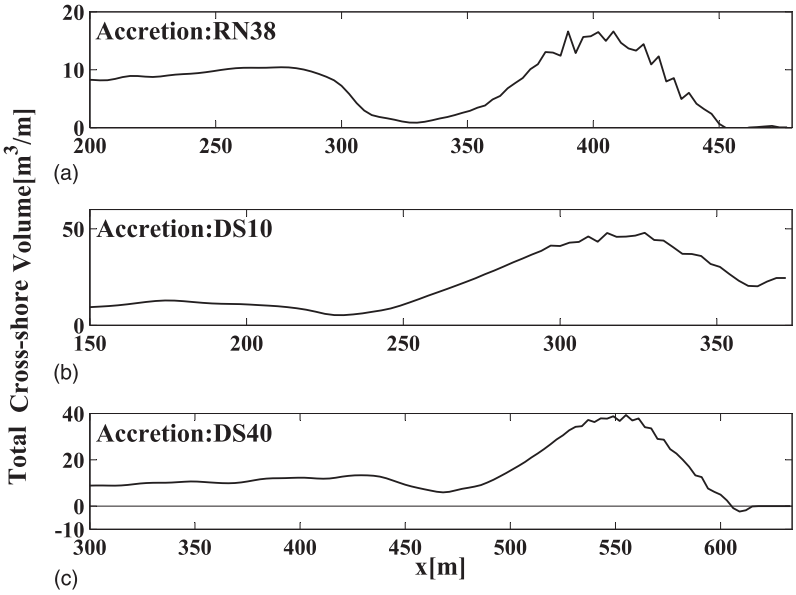

Fig. 11. Cumulative total cross-shore sand transport volume per unit width during accretion period for (a) RN38, (b) DS10, and (c) DS40

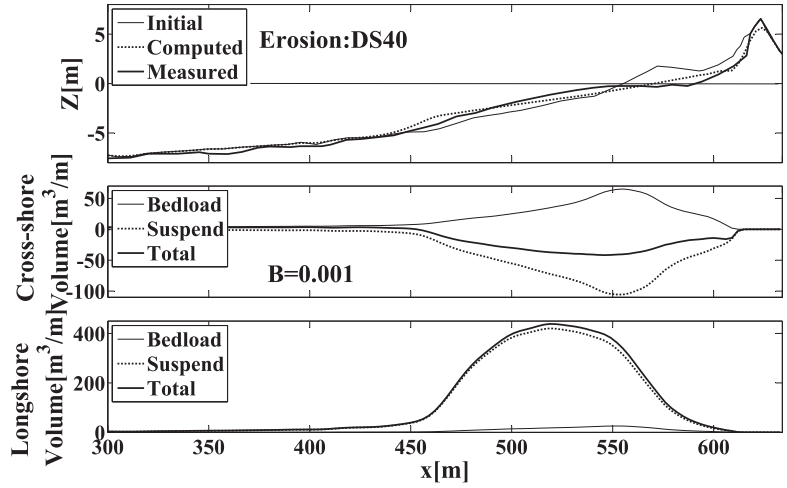

Fig. 12. Effects of reduced bed load parameter $B = 0.001$ in Fig. 5 based on $B = 0.002$

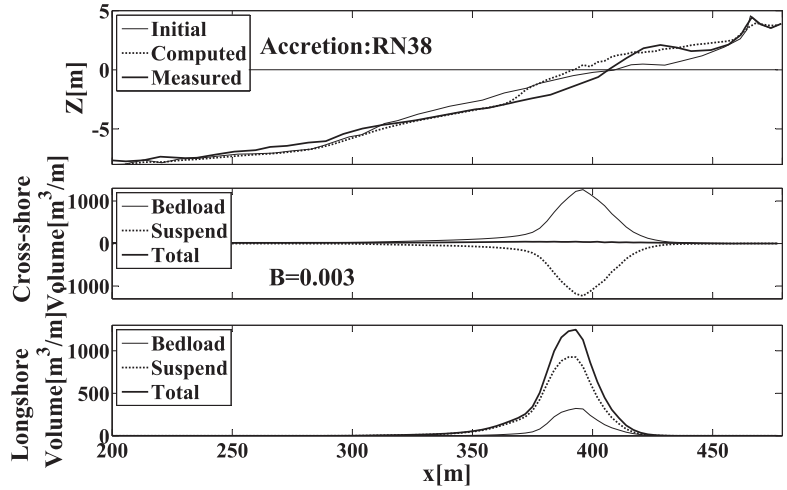

Fig. 13. Effects of increased bed-load parameter $B = 0.003$ in Fig. 8 based on $B = 0.002$

J. Waterway, Port, Coastal, Ocean Eng. 2012.138:473-483.

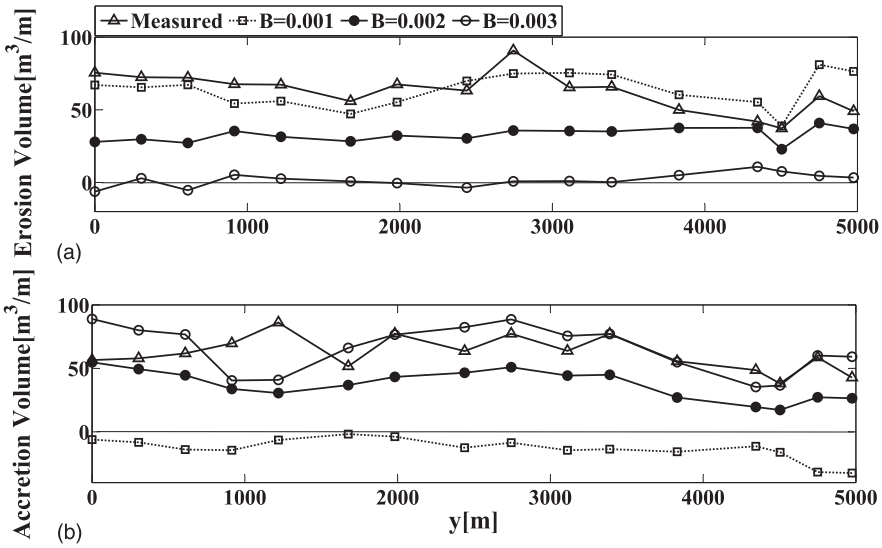

Fig. 14. Measured and computed (a) erosion and (b) accretion volumes above the mean sea level per unit alongshore length

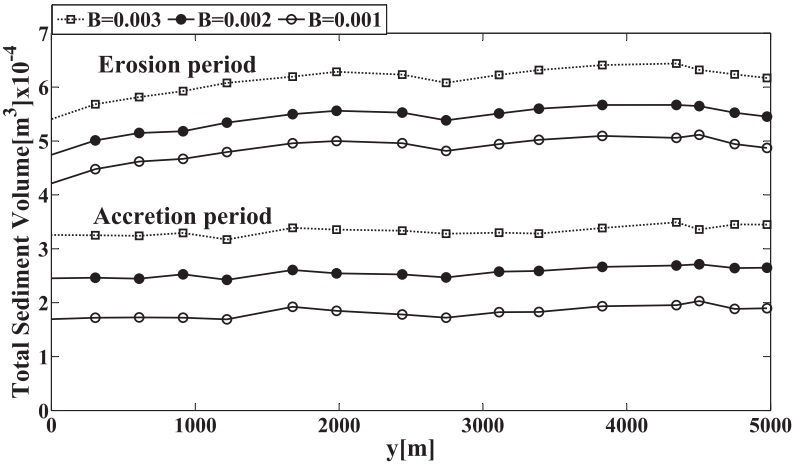

Fig. 15. Computed sand (no void) volumes transported alongshore for $B = 0.001, 0.002$, and 0.003 during erosion period (top three lines) and accretion period (bottom three lines)

major beach nourishment was initiated on these beaches in 1994. The field data are used to assess the capability and limitation of the cross-shore numerical model CSHORE for predicting both beach erosion and accretion. The CSHORE was extended to multiple cross-shore lines, and therefore the alongshore gradient of the longshore sediment transport rate in the beach profile evolution is included. The bed-load parameter b in the CSHORE was adjusted to increase b with the fraction of irregular breaking waves to reproduce the berm reconstruction above the MSL during the accretion period. The eroded and accreted profiles at 16 cross-shore lines spanning 5 km alongshore are predicted within a factor of about 2. The computed beach profile evolution was found to be affected little by the alongshore gradient of the longshore sediment transport. The total longshore sediment transport volumes computed during the erosion and accretion periods do not vary much alongshore for the present field data. The extended CSHORE will need to be compared with data with larger alongshore variations in order to assess the accuracy of the approximate method proposed for the alongshore gradient of the longshore sediment transport. Furthermore, the CSHORE will need to be verified using nourished beach data before it may be applied to improve the beach nourishment design.

Acknowledgments

This study was supported by the U.S. Army Corps of Engineers, Coastal and Hydraulics Laboratory under Contract Nos. W912HZ-10-P-0234 and W912BU-09-C-0023, as well as by the EU THESEUS Project (Innovative Technologies for Safer European Coasts in a Changing Climate). We thank Randy Wise for providing the beach profile data.

References

Anderson, D. A., Tannehill, J. C., and Pletcher, R. H. (1984). *Fluid mechanics and heat transfer*, Hemisphere, New York.

Figlus, J., and Kobayashi, N. (2008). "Inverse estimation of sand transport rates on nourished Delaware beaches." *J. Waterway, Port, Coastal, Ocean Eng.*, 134(4), 218–225.

Figlus, J., Kobayashi, N., Gralher, C., and Iranzo, V. (2011). "Wave overtopping and overwash of dunes." *J. Waterway, Port, Coastal, Ocean Eng.*, 137(1), 26–33.

Garriga, C. M., and Dalrymple, R. A. (2002). "Development of a long-term costal management plan for the Delaware Atlantic coast." *Research*

J. Waterway, Port, Coastal, Ocean Eng. 2012.138:473-483.

Rep. No. CACR-02-04, Center for Applied Coastal Research, Univ. of Delaware, Newark, DE.

Hanson, H. (1989). "GENESIS—A generalized shoreline change numerical model." *J. Coast. Res.*, 5(1), 1−27.

Jung, H., and Kobayashi, N. (2011). "Numerical modeling of erosion and recovery of Rehoboth and Dewey beaches in Delaware." *Research Rep. No. CACR-11-01*, Center for Applied Coastal Research, Univ. of Delaware, Newark, DE.

Kobayashi, N., Agarwal, A., and Johnson, B. D. (2007). "Longshore current and sediment transport on beaches." *J. Waterway, Port, Coastal, Ocean Eng.*, 133(4), 296−304.

Kobayashi, N., Buck, M., Payo, A., and Johnson, B. D. (2009). "Berm and dune erosion during a storm." *J. Waterway, Port, Coastal, Ocean Eng.*, 135(1), 1−10.

Kobayashi, N., Farhadzadeh, A., Melby, J., Johnson, B., and Gravens, M. (2010). "Wave overtopping of levees and overwash of dunes." *J. Coast. Res.*, 26(5), 888−900.

Kobayashi, N., Payo, A., and Schmied, L. (2008). "Cross-shore suspended sand and bed load transport on beaches." *J. Geophys. Res.*, 113, C07001.

Puleo, J. A. (2010). "Estimating alongshore sediment transport and the nodal point location on the Delaware-Maryland coast." *J. Waterway, Port, Coastal, Ocean Eng.*, 136(3), 135−144.

Roelvink, D., Reniers, A., van Dongeren, A., van Thiel de Vries, J., McCall, R., and Lescinski, J. (2009). "Modelling storm impacts on beaches, dunes and barrier islands." *Coast. Eng.*, 56(11−12), 1133−1152.

U.S. Army Engineer Research and Development Center. (2002). *Coastal engineering manual, Part III, Coastal sediment processes*, Coastal and Hydraulics Laboratory, Vicksburg, MS.

van Rijn, L. C. (1997). "Sediment transport and budget of the central zone of Holland." *Coast. Eng.*, 32(1), 61−90.

van Thiel de Vries, J. (2009). *Dune erosion during storm surges*, Vol. 3, Deltares Select Series, Delft, Netherlands.

Wise, R. A., Smith, S. J., and Larson, M. (1996). "SBEACH: Numerical model for simulating storm-induced beach changes. Report 4: Cross-shore transport under random waves and model validation with SUPERTANK and field data." *Tech. Rep. No. CERC-89-9*, U.S. Army Engineer Waterways Experiment Station, Vicksburg, MS.

J. Waterway, Port, Coastal, Ocean Eng. 2012.138:473-483.